Definition of [±45°]ns specimen geometry to characterize CFRP non linear shear behavior in dynamic loading

Jordan Berton, Fabien Coussa, Julien Berthe, Mathias Brieu, Eric Deletombe

Definition of $[\pm 45^\circ]_{ns}$ specimen geometry to characterize CFRP non linear shear behavior in dynamic loading

Jordan Berton*[1,2], Fabien Coussa[1], Julien Berthe[1,2], Mathias Brieu[3], Eric Deletombe[1,2]

1: ONERA-The French Aerospace Lab, F-59014, Lille Cedex, France

2: Univ Lille, CNRS, Centrale Lille UMR CNRS 9013 - LaMCube, Laboratoire de Mécanique, Multi-physique, Multi-échelle, F-59000 Lille, France

3: Department of Mechanical Engineering, California State University, Los Angeles, CA 90032, USA

*jordan.berton@onera.com

Keywords: Carbon-fibres-reinforced polymers (CFRP), shear, irreversible strain, damage

Abstract

The characterization of CFRP mechanical behavior under dynamic loading is an important topic for research laboratories. Literature reveals disparities in the evolution of shear behavior of CFRP materials under dynamic loading. Due to the lack of normative protocol for dynamic loading, these disparities can come from the geometry of the specimens used, which is generally reduced for dynamic testing. In this paper, the non-linear shear behavior of composite materials is characterized to analyse the effect of reduced geometry on the irreversible shear strain obtained compared to the reference geometry used for the quasi-static $[\pm 45^\circ]_{ns}$ tensile test. This recommendation is a first step in determining the pre-normative geometry of a $[\pm 45^\circ]_{ns}$ CFRP specimen adapted to dynamic loading.

1 Introduction

CFRP materials exhibit strain rate dependencies in particular regarding shear behavior [1]. Dynamic experimental tests can be carried out using servo-hydraulic machines [2], Split Hopkinson Pressured Bars (SHPB) [3] or more recently, the Image-Based Inertial Impact (IBII) test for high strain rates [4]. Considering results in the literature, characterization of the in-plane shear modulus may present inconsistencies in its evolution as a function of the increase in strain rate [4]. Such inconsistencies can be attributed either to the machine used for the test or the specimen's geometry. This study will focus on the use of servo-hydraulic machines for dynamic loading and the effect of the geometry sample used. Experimental tests under dynamic loading require the use of reduced geometry instead of the geometry used for quasi-static tests. This reduced geometry makes it possible to maximise the strain rate range by reducing the free length and minimising the strength by reducing the cross-section area. The choice of $[\pm 45^\circ]_{ns}$ tensile tests [5] to characterize shear behavior under dynamic loading is explained by its adaptation facility on servo-hydraulic machines compared to the Iosipescu test [6] or the rail test method [7]. By considering the whole context of the literature, this study aims to identify a reduced geometry that is as representative as possible of the standard $[\pm 45^\circ]_{ns}$ specimen and adapted to dynamic loading. The main goal of using a $[\pm 45^\circ]_{ns}$ specimen under dynamic loading is to characterize the potential effects of strain rates on the damage kinetics of CFRP material shear behavior.

$[\pm 45^\circ]_{ns}$ tensile tests have a standardized protocol to determine shear modulus [8] and maximum shear stress at failure [9]. It is well known that the $[\pm 45^\circ]_{ns}$ tensile test presents difficulties to consistently characterize the failure behavior [10]. This study will be focused on the evolution of nonlinear phenomena, hence the use of $[\pm 45^\circ]_{ns}$ specimens is considered to be reasonable. The reference specimen geometry is defined by a free length (L) of 130 mm, a width (W) of 25 mm, and a minimal thickness (T) of 2 mm. The reduction of these geometrical parameters (L, W, and T) must respect the critical cases defined in the literature. $[\pm 45^\circ]_{ns}$ tensile tests exhibit strain mapping similar to bias extension tests or picture-frame tests [11, 12, 13]. These tests define a minimal free length-to-width ratio (λ ratio) which ensures that high shear angles during loading are not dependent on the specimen geometry. The λ ratio's critical case is defined as $\lambda = 2$. Regarding thickness reduction, the critical case is defined by the symmetry induced by CFRP materials. Applied to $[\pm 45^\circ]_{ns}$ specimens, the minimal number of plies for the laminate is 4. Regarding the width, the edge effect on unidirectional composites is negligeable at double the laminate thickness for interlaminar shear stress [14].

After enumerating the importance of the various geometrical parameters in reducing the geometry, the study of literature can lead to limiting the experimental investigation's scope. A study of the viscoelastic behavior of T700/M21 CFRP does not present reduced geometry dependency on shear modulus evaluation [15]. Regarding non-linear shear behavior, no studies on CFPR materials have been found in literature. The study of Berthe et al. stressed that reduced geometry (L = 30mm, W = 15mm, and T = 4 plies [15]) does not allow the non-linear shear behavior of the reference geometry to be correctly correlated without concluding on the cause. However, a study on a 2D Glass Fiber Reinforced Polymer (GFRP) shows that the non-linear shear behavior of a $[\pm 45^\circ]_{ns}$ specimen depends on the λ ratio [16]. With the 2D GFRP used in [16], the critical case $\lambda = 2$ does not allow the non-linear shear behavior to be correctly correlated during tensile testing. Only a ratio $\lambda = 2{,}4$ guaranteed a non-linear shear behavior representative of a reduced geometry compared to the reference one. The possible origin of this geometry dependency may be attributed to the shear regions induced by the $[\pm 45^\circ]_{ns}$ specimen during tensile testing [17]. A significant reduction of the free length may increase the influence of these hybrid shear regions on load measurement.

2 Experimental procedure

This section aims to describe the experimental procedure for the analysis of the potential geometrical effects on the non-linear shear behavior of unidirectional composites. $[\pm 45^\circ]_{ns}$ specimens are defined by three geometrical parameters: free length (L), width (W), and thickness (T).

2.1 Material

T700/M21 is an unidirectional composite material with an epoxy matrix blend including thermoplastic particles [18] and reinforced by carbon fiber. The main advantage of these modified composites is that they increase durability by microcrack and crack bifurcation [19]. The $[\pm 45°]_{ns}$ specimens are manually manufactured from a unidirectional prepeg of T700/M21 (HexPly© UD/M21/35%/268/T700GC). Curing cycles are performed with an autoclave pressure system that respected the manufacturer's recommendations, which minimize the voids contents by the normalized manufacturing process. In order to minimize stress concentrations during testing, each specimens had tabs at the clamping positions (tab dimensions: 1 mm thick and 50 mm long). They are manufactured with a 2D twill-wave glass/epoxy composite.

2.2 Specimens specifications

In the sequel, we will use the following notation: L, W, T for a sample which free length is L (mm), width is W (mm) and thickness T (number of plies). The specimen geometries tested in this paper are listed in Table 1. It is only possible to reduce the standard thickness from 8 to 4 plies. Considering the limit case of the free length-to-width ratio ($\lambda = 2$) [20], the minimum free length reduction is L = 50 mm with a width of W = 25 mm (L50W25T8 specimen). The 25 mm width is defined by the standard recommendation [8]. The L55W25T8 and L60W25T8 specimens are tested to measure possible effects of the free length variation close to the λ ratio's minimum value and no more than the λ ratio identify by Coussa et al. [16]. The edge effects chosen value corresponds to a quarter of the thickness [14]. For the width reduction by considering the YFLA-2 strain gauges used in this work, the minimum admissible value is W = 15 mm. The different widths tested are the minimum value (L130W15T8) and a mid-value (L130W20T8). All these geometries are compared to the reference one: L130W25T8. Regarding the last two specimens (L104W20T8 and L78W15T8), the width variation is combined with the free length variation for two specimens. The fixed parameter is the free length-to-width ratio which is equal to the reference value ($\lambda = 5.2$) corresponding to a width of W = 20 mm with a free length of L = 104 mm. For a width of W = 15 mm, the free length is L = 78mm.

	L (mm)	W (mm)	T (Qty)
L130W25T8	130	25	8
L130W25T4	130	25	4
L60W25T8	60	25	8
L55W25T8	55	25	8
L50W25T8	50	25	8
L130W20T8	130	20	8
L130W15T8	130	15	8
L104W20T8	104	20	8
L78W15T8	78	15	8

Table 1: Specimen dimensions used for the experimental investigation

2.3 Incremental cyclic loading tensile tests

An Instron© 6837 electromechanical testing machine is used to perform the tensile tests. The load applied to the specimens is measured with the ±30 kN Instron© 2580 Series Static Load Cells. Strain is measured with strain gauges TML© YFLA-2. They are glued with TML© special glue and localized longitudinally ($\vec{xx}$) and transversely ($\vec{yy}$) to the loading axis. In accordance with standardized tests, shear strain (ε_{12}) is computed by the Equation (1): where ε_{12} is expressed with respect to the material axis and ε_{xx} and ε_{yy} with respect to the loading axis.

$$2\varepsilon_{12} = \varepsilon_{xx} - \varepsilon_{yy} \tag{1}$$

Tensile tests are performed to assure a theoritical strain-rate of $\dot{\varepsilon}$ = 3.33·10^{-4} s^{-1} for all specimen geometries. It corresponds, for the minimal free length, to 1 mm.min^{-1} of cross-head displacement. Strain and load acquisition frequency is set at f = 100 Hz. Tensile tests are run by incremental displacement which generates successive elongations up to the specimens failure. The different macroscopic variables of interest which can be defined for each cyclic displacement applied to the specimen. The end of the loading is characterized by the maximum shear stress ($\sigma_{12}^{(i)max}$) and the maximum shear strain ($\varepsilon_{12}^{(i)max}$). Irreversible shear strain ($\varepsilon_{12}^{(i)irr}$) is evaluated for each unloading phase. Elastic shear strain ($\varepsilon_{12}^{(i)elas}$) is computed by subtracting the irreversible strain from the maximum strain. As the irreversible shear strain can be small for the first displacement increment, it is required to make sure it is bigger than the noise measurement. Noise measurement is estimated by measuring the strain before loading. In this study, the noise measurement is approximately $\Delta \simeq 4.10^{-5}$. The main objective of this work is to use $[\pm 45°]_{ns}$ specimens to characterize non-linear shear behavior and its damage evolution during incremental tensile tests. Macroscopic damage variable can be evaluated using Equation (2) with a scalar variable (d_{12}) representing rigidity loss between the considered shear modulus of a loading cycle i (G_{12}^i) and the initial shear modulus G_{12}^0 [21]. The dynamic geometry will be defined by studying the geometrical parameter's effect on the macroscopic evolution of damage variable.

$$d_{12} = 1 - \frac{G_{12}^i}{G_{12}^0} \tag{2}$$

The shear modulus (G_{12}) used to calculate the damage variable can be estimated using various methods. The method proposed in [22] calculates the shear modulus considering the extremum of a solicitation increment. In [2], the method uses specific stress values ($\frac{\sigma_{12}^{max}}{2}$ and $\frac{\sigma_{12}^{max}}{10}$) to calculate the shear modulus. The method in [23] proposes to estimate the shear modulus between a pre-determined range of shear strains. Several linear regressions are calculated in this range. The linear regression giving the higher regression coefficient is then used to evaluate the shear modulus. The main advantage of this last method is that it considers a possible evolution of the required range needed to calculate the shear modulus under several strain-rates. Considering T700/M21 strain rate dependencies regarding shear behavior [15], the last method was selected for this study. The predetermined shear strain range is between ε_{12} = 0.05 % and ε_{12} = 0.2 %.

3 Results and discussion

Each test has been stopped when a crack occurred in the strain gauges which leads to an incorrect evaluation of shear strain. As a consequence, the last stress and strain value recorded are not necessarily the specimen's ultimate failure values. These early interruptions can explain the irreversible strain and maximum strain differences between two specimens of the same geometry (Table 2 and Table 3). Each strain measurement does not go beyond 7 % in order to limit the effects of fibers rotation due to the

$[\pm 45°]_{ns}$ specimen [10]. Regarding the key, a geometry is represented by a colour and a sample test by a geometric symbol (△, ◊ and ⬠). Figure 1 describes thickness reduction comparison. Figure 1a shows that the maximum shear strain has a different evolution between the two thicknesses. For $\varepsilon_{12}^{irr} \leq 0.5$ %, the specimen with reduced thickness generates a higher value of irreversible shear strain than the reference one. The maximum shear strains for $\varepsilon_{12}^{irr} \geq 0.5$ % seem to have the same linear evolution for the two thicknesses. At $\varepsilon_{12}^{max} \simeq 2$ %, the irreversible shear strain is approximately at $\varepsilon_{12}^{irr} \simeq 0.6$ % for the 8-ply specimens and $\varepsilon_{12}^{irr} \simeq 0.9$ % for the 4-ply specimens. The origin offset tends to generate a difference of 0.4 % higher value for the 4-ply specimens for $\varepsilon_{12}^{irr} \geq 0.5$ %. At $\varepsilon_{12}^{max} \simeq 4$ %, the 8-ply specimens exhibit $\varepsilon_{12}^{irr} \simeq 2$ % whereas the 4-ply specimens reach $\varepsilon_{12}^{irr} \simeq 2.4$ %. Figure 1b represents the evolution of irreversible strain as a function of maximum stress. For the same shear stress level, the 8-ply specimens generate less irreversible shear strain than the 4-ply specimens. This difference can be attributed to the early emergence of the irreversible strain for the 4-ply specimens. Maximum shear stress at failure is 20 % lower for the 4-ply specimens compared to the 8-ply specimens (Table 2). This difference can be explained by the proportion of embedded plies between the 8-ply and 4-ply specimens. The study [24] verifies that a clustered laminate has a lower *in situ* shear strength than an alternating laminate. Regarding the L130W25T4 specimens, the laminate is defined by two outer plies and two embedded plies, contrary to the L130W25T8 specimens which has alternating plies between outer and embedded plies. In addition, the study [25] shows that the *in situ* shear strength evolution of the outer or embedded plies of a CFRP laminate is equivalent when the outer ply is half of the thickness of the embedded ply. The 4-ply specimen combines the lower *in situ* shear strength of the clustered laminate with the *in situ* shear strength evolution of the outer ply equivalent to the embedded ply.

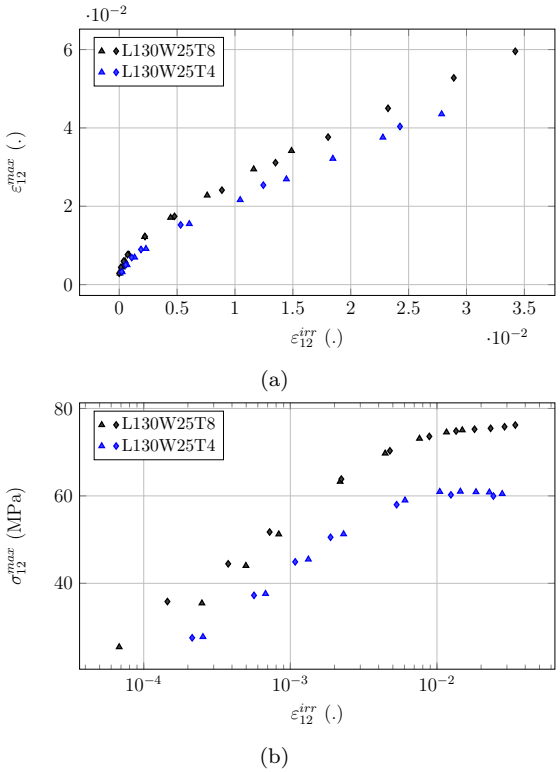

Figure 1: Evolution of the irreversible shear strain as a function of the maximum shear strain (left hand side) and the maximum shear stress (right hand side) for the thickness reduction.

	L130W25T8		L130W25T4	
Specimen	1	2	1	2
ε_{12}^{irr} (%)	1.5	3.4	2.7	2.4
ε_{12}^{max} (%)	3.4	6.0	4.3	4.0
σ_{12}^{max} (MPa)	75.0	76.2	60.5	60.0

Table 2: Evaluation of the maximum values of interest for the various thicknesses studied

Figure 2 shows the results for the variation of the free length and width. The evolution of irreversible shear strain as a function of maximum shear strain does not present macroscopic differences. In comparison with the thickness reduction, Figure 2a shows the equivalence of all geometries with the reference geometry. This is also verified by comparing the irreversible shear strain as a function of maximum shear stress with Figure 2b. The scattering for $\varepsilon_{12}^{irr} \leq 10^{-4}$ may be due to measurement noise. The difference of the maximum shear stress for each specimen is correlated with the classical dispersion of handmade composite laminates [15]. In this paper and in opposition to [16], no experimental effects of the free length and width reduction has been found regarding the studied material. The origin of this difference could be attributed to the nature of the tested material: UD ply in this study and 2D woven ply in [16]. Even if tensile test on $[\pm 45°]_{ns}$ specimens made from UD ply are classically compared to bias tests on 2D woven composite materials, the mechanisms at the origin of the different shear regions observable on the specimens are known to be different [11, 13, 20] and may explain these differences.

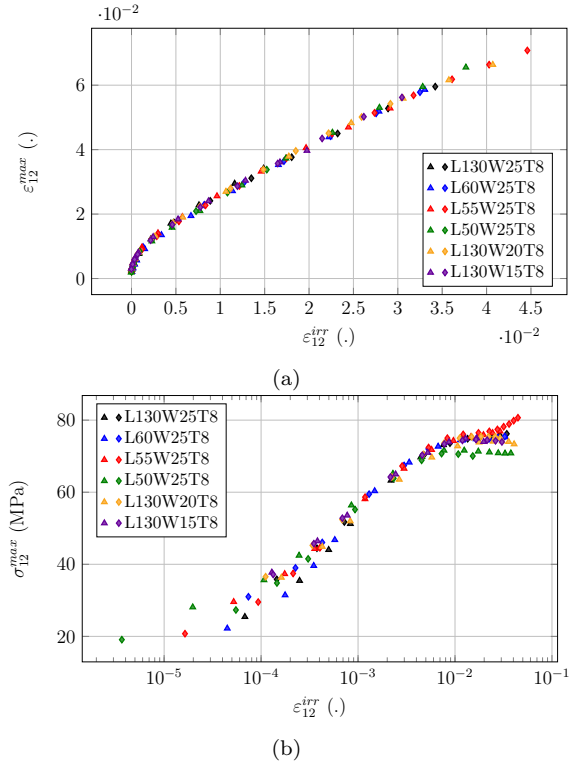

Figure 2: Evolution of the irreversible shear strain as a function of the maximum shear strain (left hand side) and the maximum shear stress (right hand side) for the free length and width reduction

	L130W25T8		L60W25T8		L55W25T8	
Specimen	1	2	1	2	1	2
ε_{12}^{irr} (%)	1.5	3.4	3.3	3.2	2.9	4.4
ε_{12}^{max} (%)	3.4	6.0	5.9	5.8	5.2	7.0
σ_{12}^{max} (MPa)	75.0	76.2	75.2	75.4	77	80.6
	L50W25T8		L130W20T8		L130W15T8	
Specimen	1	2	1	2	1	2
ε_{12}^{irr} (%)	3.7	1.5	4.0	2.9	2.0	3.0
ε_{12}^{max} (%)	6.6	3.4	6.6	5.4	4.0	5.6
σ_{12}^{max} (MPa)	70.8	70.0	73.3	75.0	74.0	74.0

Table 3: Evaluation of the maximum values of interest for the free length and the width reduction

Figure 3 and Figure 4 compare damage kinetics. The evolution of macroscopic damage is calculated as a function of irreversible strain for the free length values in Figure 3a. The combination of free length and width variations is presented in Figure 3b. This analysis is focused on irreversible strain smaller than $\varepsilon_{12}^{irr} \leq 1$ % in order to avoid potential disparities due to material manufacturing. This allows us to observe a possible geometry effect on the emergence and evolution of macroscopic damage as a function of irreversible deformations. The L50W25T8 specimen has a different evolution and a higher scattering compared to the others (Figure 3a). Furthermore, the L78W15T8 specimen has a higher scattering than L130W25T8 and L104W20T8 specimens (Figure 3b). Table 4 presents the three macroscopic damage values close to $\varepsilon_{12}^{irr} \simeq 1$ % for the combined free length and width variation.

Figure 4 compares the evolution of the macroscopic damage variable as a function of the irreversible shear strain for the different length values. For $d_{12} \leq 0.04$, the three specimens have a similar evolution. Hence, they are concatenated for $d_{12} \geq 0.04$. A linear regression is computed for each geometry in order to quantify the damage kinetics. The results of each linear regression are listed in the Table 5. The L50W25T8 specimen has an evolution 21 % higher than the reference specimen. L60W25T8 and L55W25T8 respectively have 3 % and 0.5 % slope difference. The correlation coefficient (R^2) represents the closeness of the data to the fitted regression line. It is therefore a reliable value for exhibiting the scattering of concatenated tests. In addition to slope differences, the L50W25T8 specimen also has higher scattering than the reference specimen and the free length reductions of the others.

Given the analysis of damage kinetics, it seems that the critical case of geometrical parameter reduction ($\lambda = 2$ and W = 15 mm) exhibits differences with the reference specimen. This wide experimental study shows that the minimum geometrical parameters guaranteeing the representativity with the reference geometry are: $\lambda = 2.2$, W = 20 mm and T = 8 plies.

4 Conclusion

The effect of the $[\pm 45°]_{ns}$ CFRP specimen's geometrical parameters on non-linear shear behavior was studied in this paper. First, this paper investigated the thickness, free length, and width reduction separately. The results demonstrate a decrease of 20 % of the maximum shear stress at failure for the 4-ply specimens compared to the 8-ply. The variation of the free length and the width did not show any difference when compared to the reference specimen. Then, the investigation focused on the evolution of macroscopic damage. Width reduction was combined with the free length reduction to increase the analysis range. The results show that the critical cases of geometry reduction could affect macroscopic damage calculation by increasing scattering and by modifying macroscopic damage kinetics for $\varepsilon_{12}^{irr} \leq 1$ %. This wide experimental investigation allowed us to define the smallest geometry that guarantees the representativeness of the reference specimen.

This suitable geometry is defined by: $\lambda = 2.2$, width = 20 mm and thickness = 8 plies (for the T700/M21 unidirectional composite).

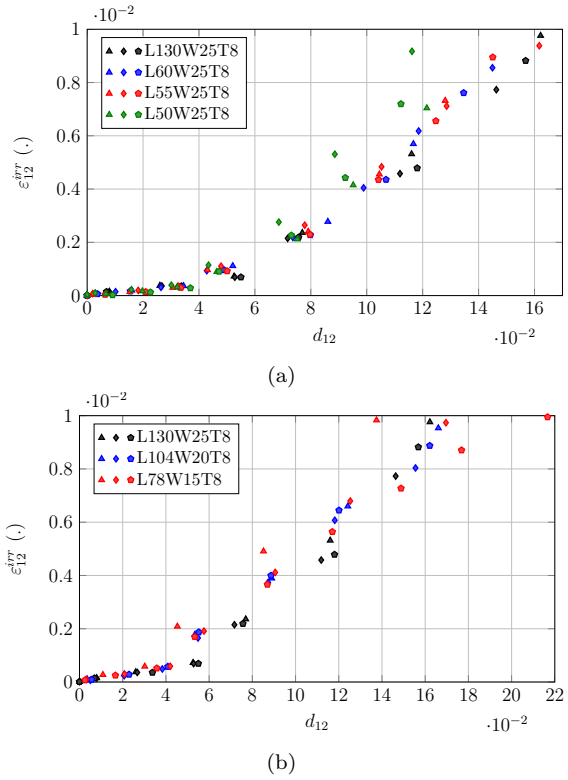

Figure 3: Evolution of the macroscopic damage as a function of the irreversible shear strain for free length variation (left hand side) and the width variations with the λ ratio fixed to the standard value (right hand side)

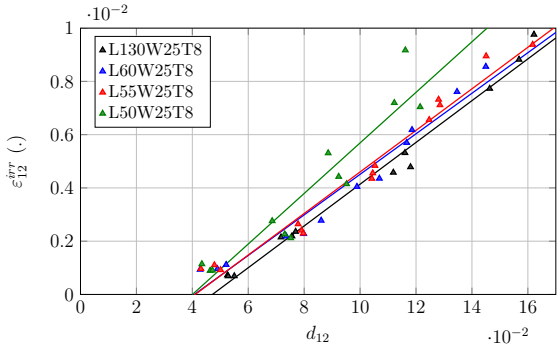

Figure 4: Computation of the linear regression of the irreversible shear strain for $d_{12} > 0.04$

	L130W25T8			L104W20T8			L78W15T8		
Specimen	1	2	3	1	2	3	1	2	3
d_{12}	0.16	0.15	0.16	0.17	0.16	0.16	0.14	0.17	0.22

Table 4: Results for the combinaison of the free length and width reduction for $\varepsilon_{12}^{irr} \simeq 1$ %

	L130W25T8	L60W25T8	L55W25T8	L50W25T8
Slope	0.0784	0.0761	0.0780	0.0949
R^2	0.9857	0.9592	0.9692	0.8877

Table 5: Linear regression parameters for the length reduction

Acknowledgements

The authors thank Onera Centre de Lille and the Haut de France Region for Ph.D. funding.

References

[1] A. Kidane, H. Gowtham, and N. Naik, "Strain rate effects in polymer matrix composites under shear loading: A critical review." *J. dynamic behavior mater.*, vol. 3, pp. 110–132, 2017. [Online]. Available: https://doi.org/10.1007/s40870-017-0098-2

[2] J. Fitoussi and al., "Experimental methodology for high strain-rates tensile behaviour analysis of polymer matrix composites," *Composites Science and Technology*, vol. 65, no. 14, pp. 2174 – 2188, 2005. [Online]. Available: https://doi.org/10.1016/j.compscitech.2005.05.001

[3] H. Kolsky, "An investigation of the mechanical properties of materials at very high rates of loading," *Proceedings of the Physical Society. Section B*, vol. 62, no. 11, pp. 676–700, nov 1949. [Online]. Available: https://doi.org/10.1088%2F0370-1301%2F62%2F11%2F302

[4] S. Parry, L. Fletcher, and F. Pierron, "The off-axis ibii test for composites," *J. dynamic behavior mater*, vol. 7, pp. 127–155, 2021. [Online]. Available: https://doi.org/10.1007/s40870-020-00271-7

[5] B. W. Rosen, "A simple procedure for experimental determination of the longitudinal shear modulus of unidirectional composites," *Journal of Composite Materials*, vol. 6, no. 3, pp. 552–554, 1972. [Online]. Available: https://doi.org/10.1177/002199837200600310

[6] N. Iosipescu, "New accurate procedure for single shear testing of metals," *J Mater*, vol. 2, pp. 537–566, 1967. [Online]. Available: https://ci.nii.ac.jp/naid/10006135450/en/

[7] J. Whitney and al., "Analysis of the rail shear test-applications and limitations," *J. of C. Materials*, 1971. [Online]. Available: https://doi.org/10.1177/002199837100500103

[8] DIN-EN-ISO-14129, "Determination of the in-plane shear stress/shear strain response, including the in-plane shear modulus and strength, by the 45 tension test method," *European Committee for Standardization*, 1997.

[9] AITM-1-0002, "Determination of in-plane shear properties," vol. Issue 3, pp. 1–11, 1998.

[10] M. R. Wisnom, "The effect of fibre rotation in ±45° tension tests on measured shear properties," *Composites*, vol. 26, no. 1, pp. 25–32, 1995. [Online]. Available: https://www.sciencedirect.com/science/article/pii/0010436194P3626C

[11] K. Potter, "Bias extension measurements on cross-plied unidirectional prepreg," *Composites Part A: Applied Science and Manufacturing*, vol. 33, no. 1, pp. 63 – 73, 2002. [Online]. Available: http://www.sciencedirect.com/science/article/pii/S1359835X01000574

[12] G. Lebrun, M. N. Bureau, and J. Denault, "Evaluation of bias-extension and picture-frame test methods for the measurement of intraply shear properties of pp/glass commingled fabrics," *Composite Structures*, vol. 61, no. 4, pp. 341 – 352, 2003, selected Papers from the Symposium on Design and Manufacturing of Composites. [Online]. Available: http://www.sciencedirect.com/science/article/pii/S0263822303000576

[13] F. Härtel and P. Harrison, "Evaluation of normalisation methods for uniaxial bias extension tests on engineering fabrics," *Composites Part A: Applied Science and Manufacturing*, vol. 67, pp. 61 – 69, 2014. [Online]. Available: http://www.sciencedirect.com/science/article/pii/S1359835X14002449

[14] R. B. Pipes and N. J. Pagano, *Interlaminar Stresses in Composite Laminates Under Uniform Axial Extension*. Dordrecht: Springer Netherlands, 1994, ch. 5, pp. 234–245. [Online]. Available: https://doi.org/10.1007/978-94-017-2233-9_19

[15] J. Berthe, M. Brieu, E. Deletombe, G. Portemont, P. Lecomte-Grosbras, and A. Deudon, "Consistent identification of cfrp viscoelastic models from creep to dynamic loadings," *Strain*, vol. 49, no. 3, pp. 257–266, 2013. [Online]. Available: https://onlinelibrary.wiley.com/doi/abs/10.1111/str.12033

[16] F. Coussa and al., "A consistent experimental protocol for the strain rate characterization of thermoplastic fabrics," *Strain*, vol. 53, no. 3, p. e12220, 2017, e12220 10.1111/str.12220. [Online]. Available: https://onlinelibrary.wiley.com/doi/abs/10.1111/str.12220

[17] P. Harrison, M. Clifford, and A. Long, "Shear characterisation of viscous woven textile composites: a comparison between picture frame and bias extension experiments," *Composites Science and Technology*, vol. 64, no. 10, pp. 1453–1465, 2004. [Online]. Available: https://www.sciencedirect.com/science/article/pii/S0266353803004007

[18] D. Tilbrook, D. Blair, M. Boyle, and P. Mackenzie, "Composite materials with blend of thermoplastic particles," DUBLIN, CA US patentus 20 080 286 578, 2008. [Online]. Available: http://www.faqs.org/patents/app/20080286578

[19] R. A. Pearson and A. F. Yee, "Toughening mechanisms in thermoplastic-modified epoxies: 1. modification using poly(phenylene oxide)," *Polymer*, vol. 34, no. 17, pp. 3658–3670, 1993. [Online]. Available: https://www.sciencedirect.com/science/article/pii/003238619390051B

[20] J. Wang, J. Page, and R. Paton, "Experimental investigation of the draping properties of reinforcement fabrics," *Composites Science and Technology*, vol. 58, no. 2, pp. 229–237, 1998, australasian Special Issue on Manufacturing Processes and Mechanical Properties Characterisation of Advanced Composites. [Online]. Available: https://www.sciencedirect.com/science/article/pii/S0266353897001152

[21] P. Ladeveze and E. LeDantec, "Damage modelling of the elementary ply for laminated composites," *Composites Science and Technology*, vol. 43, no. 3, pp. 257–267, 1992. [Online]. Available: https://www.sciencedirect.com/science/article/pii/026635389290097M

[22] J.-L. C. J. Lemaitre, *Mécanique des matériaux solides*, Dunod, Ed., 1985.

[23] M. Castres, "Modélisation dynamique avancée des composites à matrice organique (cmo) pour l'étude de la vulnérabilité des structures aéronautiques," Ph.D. dissertation, Ecole Centrale de Lille, 2018.

[24] F.-K. Chang and M.-H. Chen, "The in situ ply shear strength distributions in graphite/epoxy laminated composites," *Journal of Composite Materials*, vol. 21, no. 8, pp. 708–733, 1987. [Online]. Available: https://doi.org/10.1177/002199838702100802

[25] P. P. Camanho, C. G. Dávila, S. T. Pinho, L. Iannucci, and P. Robinson, "Prediction of in situ strengths and matrix cracking in composites under transverse tension and in-plane shear," *Composites Part A: Applied Science and Manufacturing*, vol. 37, no. 2, pp. 165–176, 2006, compTest 2004. [Online]. Available: https://www.sciencedirect.com/science/article/pii/S1359835X05002526